Electron paramagnetic resonance study of a new centre and eight new sites of Fe^{3+} ions in $KTiOPO_4$

1998 J. Phys.: Condens. Matter 10 341

(http://iopscience.iop.org/0953-8984/10/2/013)

J. Phys.: Condens. Matter **10** (1998) 341–348. Printed in the UK PII: S0953-8984(98)87512-7

Electron paramagnetic resonance study of a new centre and eight new sites of Fe^{3+} ions in $KTiOPO_4$

Sang Won Ahn† and Sung Ho Choh‡

Department of Physics, Korea University, Seoul 136-701, Republic of Korea

Received 8 September 1997, in final form 21 October 1997

Abstract. Careful reanalysis of EPR spectra of Fe^{3+} ions in $KTiOPO_4$ (KTP) has been carried out in order to resolve the weaker lines not considered in our previous study. Eight additional sets of fine-structure (FS) lines, CYj ($Y = 3, 4$ and $j =$ a, b, c, d), have now been identified and their respective spin-Hamiltonian parameters have been determined. These sets are classified into two groups denoted as centres C3 and C4, each of which yields identical principal values of the **g** tensor and second-order zero-field splitting tensor but different orientations of the principal axes. For four sets of FSs belonging to each centre, the direction cosines of the principal axes are found to be $lmn, \bar{l}mn, l\bar{m}n$, and $\bar{l}\bar{m}n$, consistently with the crystal symmetry of KTP. The FS C4a agrees well with that denoted as the centre ST4 by other investigators, whereas the others are newly identified. The eight magnetically inequivalent Fe^{3+} sites are assigned to two titanium sites: Ti(1) and Ti(2). Two different centres, C1 and C3 as well as C2 and C4, arising from Fe^{3+} ions at the respective Ti(1) and Ti(2) sites, are explained by differing charge compensation. It is also suggested that a vacancy of the first-neighbour oxygen OT(1), denoted as $V_{OT(1)}$, plays the role of a divalent positive charge compensator simultaneously for two Fe^{3+} ions at the adjacent Ti(1) and Ti(2) sites.

1. Introduction

Potassium titanyl phosphate $KTiOPO_4$ (KTP) crystallizes in the orthorhombic space group $Pna2_1$ with eight formula units per unit cell [1, 2]. The structure exhibits two crystallographically different titanium sites: Ti(1) and Ti(2), replaced by Fe^{3+} ions [3–5]. Each of the titaniums has four chemically equivalent but magnetically inequivalent sites due to the symmetry elements of KTP crystal, characterized by two glide planes n and a, and one screw axis 2_1 [6–8].

In the present study, from a careful reanalysis of EPR spectra of Fe^{3+} ions in KTP, we have been able to identify two additional Fe^{3+} centres denoted as C3 and C4 with relatively weaker lines. Thus all four sets of fine-structure (FS) lines, CYj ($Y = 3$, 4 and $j =$ a, b, c, d), arising from Fe^{3+} ions at four magnetically inequivalent Ti sites for each centre, are classified, and consequently eight new Fe^{3+} sites are determined. Possible charge-compensation models for two different centres arising from Fe^{3+} ions at each of the Ti sites are also discussed.

† Present address: Department of Chemistry, University of Houston, Houston, TX 77204-5641, USA.
‡ To whom any correspondence should be addressed.

0953-8984/98/020341+08$19.50

2. Experiments

KTP crystals doped with 0.01 mol% of Fe were synthesized by the flux method using the chemical $K_6P_4O_{13}$ [9], known as a particularly suitable flux for growing KTP crystals [10]. EPR measurements have been carried out at room temperature by employing a Bruker Q-band spectrometer (ESP 300 series) with 100 kHz modulation at the Seoul Branch of the Korea Basic Science Institute. The crystal, oriented by the x-ray Laue method, was fixed to its holder before it was mounted inside the cavity. Two sets of FS lines became degenerate and merged into one set when the magnetic field $\boldsymbol{B}$ was aligned in each of the planes ab, bc, and ca. This made it possible to establish crystal alignments within $\pm 0.05^\circ$ in the three planes by adjusting the crystal orientation inside the cylindrical cavity in such a way as to achieve the degeneracy of the EPR lines [6, 7]. EPR spectra were recorded by varying the orientations of $\boldsymbol{B}$ in the three planes with the polar angle θ and the azimuth angle ϕ (measured from the $+c$- and $+a$-axis, respectively) ranging from 0° to 180°. The frequencies were kept in the range ± 0.0003 GHz during the measurements, at 33.8673, 33.8647, and 33.8616 GHz, in the planes ab, bc, and ca, respectively [7].

3. Results and discussion

For analysis of EPR spectra and their angular dependence for Fe^{3+} ions with the effective spin $S = 5/2$ at arbitrary low-symmetry sites, the appropriate spin Hamiltonian is given by [3–5, 7]

$$H_S = \sum_{ij} \mu_B B_i g_{ij} S_j + \sum_{m=-2}^{2} B_2^m O_2^m + \sum_{m=-4}^{4} B_4^m O_4^m \tag{1}$$

where six independent elements, g_{ij}, for the $\mathbf{g}$ tensor, five for the second-order zero-field splitting (ZFS) tensor, and nine for the fourth-order ZFS tensor are needed to describe the spectra arising from Fe^{3+} ions located at triclinic symmetry sites in KTP. The higher-order Zeeman terms of the type S^3B and SB^3 may in general be included in H_S in equation (1) [11]. However, since the number of adjustable parameters for triclinic symmetry would be prohibitive for a meaningful fitting and the magnitude of these parameters is expected to be very small, we refrain from taking these terms into account. For all FSs the 20 parameters of equation (1) were calculated by employing a computer program, EPR-NMR [11].

A typical EPR spectrum of the Fe^{3+} ion in KTP for $\boldsymbol{B}$ parallel to the orientation of $\theta = 27^\circ$ and $\phi = 0^\circ$ is depicted in figure 1, where all of the EPR lines are twofold degenerate. The possible hyperfine splitting of the lines due to the ^{57}Fe isotope ($I = 1/2$, natural abundance $\approx$2.15%) is not resolved in our spectra, whereas the spectra consist of eight sets of well resolved FS lines for this orientation. EPR lines with strong intensities have been assigned to the centres C1 and C2 in our previous report [7], whereas those with much weaker intensities have now been classified, and assigned to the centres C3 and C4. From the angular dependence of the EPR spectra, three allowed ($\Delta M_S = \pm 1$) and two quasi-forbidden transitions ($\Delta M_S = \pm 2$) between six spin states due to the effective spin $S = 5/2$ were identified in the planes ab, bc, and ca, where two sets of FS lines became degenerate and merged into one set. The degenerate pairs are different in each of the three planes, whose aspects are the same as those observed for EPR lines of Cr^{3+} in KTP [6, 8]. The nondegenerate pairs have mirror symmetry about the axes a, b, and c in each of the three planes. All four sets merge into one when $\boldsymbol{B}$ is aligned along each of the axes a, b, and c (see figures 2 and 3 of [7]). However, the degenerate EPR lines were split in the three skew planes, which deviated from the three planes ab, bc, and ca.

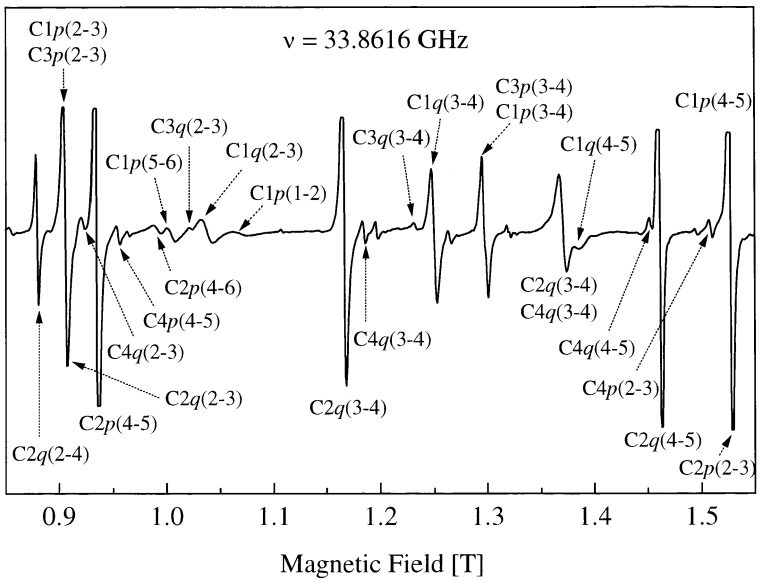

Figure 1. The first-derivative EPR spectrum of the Fe^{3+} centres, CY (Y = 1, 2, 3, and 4), in $KTiOPO_4$ measured with the Q band at room temperature for the magnetic field aligned along the orientation of $\theta = 27^\circ$ and $\phi = 0^\circ$. The pairs of numbers given in parentheses indicate the transitions between the M_S spin states $5/2, 3/2, 1/2, -1/2, -3/2$, and $-5/2$ numbered from 1 to 6, respectively. Two sets of FS lines CYp (p = a and c) as well as CYq (q = b and d) are twofold degenerate for this orientation and in the ca-plane.

Table 1. Relative orientations of the principal axes of the **g** tensor and the second-order ZFS tensor for the fine structures arising from four magnetically inequivalent Fe^{3+} sites belonging to each centre, and those of four chemically equivalent Ti sites. The orientation of the principal axes of the second-order ZFS tensor for the three other FSs for each centre can be obtained from those for the representative ones C3a and C4a in table 4—see later. The sites II, III, and IV for each of Ti(1) and Ti(2) can be obtained by applying the respective reflection operation to the site I.

	Fine structures				Orientations (deg) of the principal axes		Reflection
Ti sites	C1	C2	C3	C4	θ	ϕ	planes
I	C1a	C2a	C3a	C4a	θ_{CYa}	ϕ_{CYa}	
II	C1b	C2b	C3b	C4b	θ_{CYa}	$180^\circ - \phi_{CYa}$	n
III	C1c	C2c	C3c	C4c	θ_{CYa}	$360^\circ - \phi_{CYa}$	a
IV	C1d	C2d	C3d	C4d	θ_{CYa}	$180^\circ + \phi_{CYa}$	n, a

Since there are two possibilities for choosing a set of the FS lines corresponding to a specific Fe^{3+} site in each of the planes ab, bc, and ca, there are eight different ways to assign a set of the FS lines arising from one Fe^{3+} site in the three planes (see figures 2 and 3 of [7]). The agreement of the calculated EPR line positions with experimental ones is excellent for four particular choices of the FS lines, while it fails completely for the other four choices. The four sets corresponding to the 'good' choices have been denoted as CYj (j = a, b, c, d) for a given centre CY (Y = 3 and 4). The four sets yield identical principal

Table 2. Degenerate pairs of four sets of fine-structure lines for each centre CY (Y = 1, 2, 3, and 4) with an applied magnetic field in the planes ab, bc, and ca, and identical pairs, to four chemically equivalent Ti sites for each of Ti(1) and Ti(2).

Planes	Fine structures		Ti sites	
ab	[CYa, CYd]	[CYb, CYc]	[I, IV]	[II, III]
bc	[CYa, CYb]	[CYc, CYd]	[I, II]	[III, IV]
ca	[CYa, CYc]	[CYb, CYd]	[I, III]	[II, IV]

Table 3. Spin-Hamiltonian parameters of the representative fine structures C3a and C4a for the Fe^{3+} ions in KTP with the crystallographic axes X, Y, Z. The data of other investigators are included for comparison.

	Present work		Reference [5]	
	C3 (C3a)	C4 (C4a)	ST1	ST4
ij	Matrix components g_{ij}[a]			
XX	2.0038	2.0048	1.9997	2.0027
YY	2.0005	2.0046	2.0037	2.0045
ZZ	2.0048	2.0067	2.0038	2.0048
XY	0.0019	0.0050	−0.0015	0.0037
XZ	−0.0039	0.0009	0.0003	0.0006
YZ	−0.0019	−0.0007	−0.0001	0.0001
m	Second-order ZFS parameters B_2^m (cm^{-4})[b]			
0	283.3	192.0	265.1	200.3
1	401.6	−2164.6	1088.1	−2151.2
−1	−2376.3	623.8	−1158.7	612.1
2	714.0	−591.8	475.3	−586.1
−2	−64.4	−376.8	−219.3	−381.1
m	Fourth-order ZFS parameters 60 B_4^m (cm^{-4})[b]			
0	29.4	25.8	32.0	24.4
1	47.8	27.2	15.2	46.2
−1	86.5	15.1	63.3	24.0
2	−252.4	299.1	−304.1	254.5
−2	−34.6	77.1	−55.0	83.6
3	−1.2	−271.0	36.8	−192.4
−3	380.3	−50.8	386.5	−48.5
4	−146.9	−101.3	−167.4	−106.5
−4	−69.8	−91.3	−17.8	−96.4

[a] The estimated statistical uncertainties are ±0.0004 for all centres.
[b] The estimated maximum uncertainties of B_2^m and 60 B_4^m are ±1.3 for all centres.

values of the **g** tensor and the second-order ZFS tensor, whereas the orientations of the principal axes are different for each set. The direction cosines of the principal axes for the four sets are found to be lmn, $\bar{l}mn$, $l\bar{m}n$, and $\bar{l}\bar{m}n$. However, their relative orientations are given in terms of the polar angle θ and azimuthal angle ϕ in table 1, where those of four chemically equivalent Ti sites denoted as I–IV [6, 7] for each of Ti(1) and Ti(2), replaced by Fe^{3+} ions [3–5], are also listed. Such relationships arise from the fact that the distinction of lattice translations in the space group $Pna2_1$ can be ignored; i.e. the glide planes n and a

can be considered as mirror planes, and the twofold screw axis 2_1 as a twofold rotation axis, when $\boldsymbol{B}$ is aligned in each crystallographic plane [7]. This also gives rise to the degenerate aspects of EPR lines due to Fe^{3+} ions at two pairs of Ti sites, identical with respect to the magnetic field. Such pairs in each of the planes ab, bc, and ca are listed in table 2. The four sets of the FS lines belonging to centres C3 and C4 have now been classified, and conform well with the symmetry elements of KTP crystal.

The rotation matrices [11, 12], which transform the data for all symmetry-related sites into those for a reference site, could be found with the relations given in table 1. To obtain an accurate and meaningful determination of the spin-Hamiltonian parameters, a simultaneous fitting of all of the data for the four sets of FS lines due to magnetically inequivalent Fe^{3+} sites has been carried out using a set of the rotation matrices. The final values of g_{ij} and of the ZFS parameters for the FSs, C3a and C4a, are listed in table 3 together with the data of other investigators [5] for comparison. These parameters are given in the reference frame of the crystallographic axes system defined as $X = a = 12.814$ Å, $Y = b = 6.404$ Å, and $Z = c = 10.616$ Å. The root mean square deviation between the experimental and calculated magnetic transitions is about 1.3 mT for each centre.

The principal values of the second-order ZFS tensors and the orientations of the principal axes (x, y, z) with respect to the crystallographic axes are listed in table 4 together with those of [5, 7] for the purposes of comparison and further discussion. The principal-axis systems have been chosen to conform with the standardization convention [13, 14], i.e. $|B_2^0| \geqslant |B_2^2|$ and the two parameters have the same sign. The norm whose values are listed in table 4 is defined in terms of extended Stevens parameters as [13–15]

$$N_2 = (B_2^0)^2 + \frac{1}{3}(B_2^2)^2. \tag{2}$$

Since the norm is invariant under arbitrary rotations of the frame of coordinates, it is very useful to examine the equivalencies between the centres represented in various coordinate systems. Although the norms of C1 and C2 are very similar to those of C3 and C4, respectively, all of them are in fact different centres. The evidence can be obtained by a consideration of the conspicuously different intensities of the two centres (see figure 1) and is provided by the fact that all four sets of FS lines for each of the four centres were completely split in the three skew planes. Comparison of the values of N_2 for the centres reported in [5] and for the centres in table 4 reveals that C4a is very similar to ST4 whereas C3a and ST1 are different. The norms of the centres C1 with comparatively stronger intensities and C3 with weaker intensities are too similar for one to determine which centre corresponds to ST3 ($N_2 = 0.007\,41$ cm^{-2}) by just comparing the norms themselves. However, a comparison of the values of g_{ij} and $B_4^m O_4^m$ for the centres C1 in table 4 of [5] and C3 in table 3 makes it possible to reach the conclusion that the centre C1 rather than C3 corresponds directly to ST3. However, the centre C3 is new, and could not be matched with the centres reported previously in the literature [3–5, 7]. The centre ST1 of [5] could not correspond to any of the four centres identified in the present spectra.

Using the pseudosymmetry-axes method [16, 17], it was determined that the centres were due to the Fe^{3+} ion at Ti(1) for ST1 and ST3, and at Ti(2) for ST2 ($N_2 = 0.006\,14$ cm^{-2}) and ST4 [5]. From the similarity between the centres C3 and ST1 as well as C4 and ST4, we can conclude that C3 and C4 are due to the Fe^{3+} ion at Ti(1) and at Ti(2), respectively. As an overall consequence of the analysis of the present EPR results and those of [7] indicating that C1 and C2 arise from Fe^{3+} ions at Ti(1) and Ti(2) sites, respectively, the following can be proposed. The FSs CPa, CPb, CPc, and CPd ($P = 1, 3$) are due to the Fe^{3+} ions replacing Ti(1) ions located at the respective positions I, II, III, and IV. The FSs CQa,

Table 4. Principal values of the second-order ZFS tensors and orientations of their principal axes x, y, z with respect to the crystallographic axes X, Y, Z for the representative fine structures C3a and C4a for the Fe^{3+} ions in KTP. The data of [5, 7] are included for the purposes of comparison and discussion.

	Present work				Reference [7]			
	C3 (C3a)		C4 (C4a)		C1 (C1a)		C2 (C2a)	
Principal values of the second-order ZFS tensors[a]								
B_2^0 (cm^{-1})	−0.081 93		−0.072 25		−0.081 73		−0.073 91	
B_2^2 (cm^{-1})	−0.043 98		−0.055 29		−0.044 31		−0.044 22	
$\lambda = B_2^2/B_2^0$	0.538		0.765		0.542		0.598	
N_2 (cm^{-2})	0.007 36		0.006 24		0.007 33		0.006 12	
Orientations (deg) of the principal axes of the second-order ZFS tensors[b]								
	θ	ϕ	θ	ϕ	θ	ϕ	θ	ϕ
Ox	101.83	7.73	116.74	79.43	102.17	7.99	112.16	78.15
Oy	148.81	117.97	42.01	135.41	148.58	118.65	39.99	139.09
Oz	61.60	91.22	60.31	6.13	61.52	91.28	58.65	2.51
	Reference [5]							
	ST1		ST4					
Principal values of the second-order ZFS tensors[a]								
B_2^0 (cm^{-1})	0.055 98		−0.071 92					
B_2^2 (cm^{-1})	0.038 33		−0.055 47					
$\lambda = B_2^2/B_2^0$	0.685		0.771					
N_2 (cm^{-2})	0.003 62		0.006 20					
Orientations (deg) of the principal axes of the second-order ZFS tensors[b]								
	θ	ϕ	θ	ϕ				
Ox	120.5	12.6	116.6	80.2				
Oy	68.8	89.6	41.6	135.9				
Oz	141.8	150.0	60.6	6.5				

[a] The estimated maximum uncertainties are ±0.00012 for all centres.
[b] The estimated maximum uncertainties in the angle are ±0.05 for all centres.

CQb, CQc, and CQd ($Q = 2, 4$) are due to the Fe^{3+} sites replacing Ti(2) ions located at the respective positions I, II, III, and IV. Hence a comprehensive assignment of all sixteen Fe^{3+} EPR spectra including eight analysed previously [7] to the crystallographic sites is now achieved.

The principal axes of the second-order ZFS tensors nearly coincide for the two centres, C1 and C3 as well as C2 and C4, but their principal values differ slightly. For an explanation as to why such kinds of pairs of centres arise from the crystallographically equivalent Ti sites, possible models are illustrated in figure 2. The OT(1) oxygen ion bridges two crystallographically distinct Ti(1) and Ti(2) ions, which provide long and short bonds to

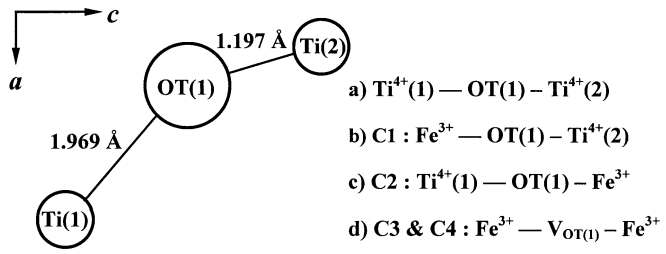

Figure 2. The projection of the chain (a) Ti(1)–OT(1)–Ti(2) on the *ca*-plane in KTP. Possible substitutional Fe^{3+} sites are suggested as follows: (b) Fe^{3+} at Ti(1) and Ti^{4+} at Ti(2) for C1, (c) Ti^{4+} at Ti(1) and Fe^{3+} at Ti(2) for C2, and (d) Fe^{3+} at Ti(1) and Fe^{3+} at Ti(2) for C3 and C4, respectively. In the structure (d), a vacancy of the oxygen OT(1) denoted as $V_{OT(1)}$ plays the role of a divalent positive charge compensator for both of the centres C3 and C4.

OT(1), respectively. The Ti(1)–OT(1)–Ti(2) chain is one of four chemically equivalent but magnetically inequivalent chains existing in the unit cell, where each of two representative FSs, C1a and C3a as well as C2a and C4a, can correspond to the Ti(1) and Ti(2) ions at position I, respectively. These representative FSs will be considered as centres in the following discussion, since the relations among the four sets of FSs belonging to each centre have been clarified in previous paragraphs.

Each of two centres, C1 and C3 as well as C2 and C4, with similar orientations of their principal axes appears likely to be arising from Fe^{3+} ions at similar structures, (b) and (d) as well as (c) and (d), respectively, in figure 2. On the other hand, the slightly different principal values might be due to the difference between the crystal fields of two Fe^{3+} ions affected by their ligands. The populations of Fe^{3+} ions substituted simultaneously for both of the Ti sites (case (d)) might be much less than those of Fe^{3+} substituted for either one of the Ti(1) and Ti(2) sites (cases (b) and (c), respectively). The centres C1 and C2 with the comparatively stronger intensity appear to be originating from such a majority of Fe^{3+} ions in the structures (b) and (c), respectively. The ionic radius of Ti^{4+} (0.68 Å) is very similar to that of Fe^{3+} (0.64 Å), but the charge states of the two ions are different. When the Fe^{3+} ion substitutes for the Ti site, this defect centre should be compensated by a monovalent cation for each Fe^{3+} ion. It is difficult to determine the charge compensator and its location for each centre from the present data alone, since there exist several ions with monovalent charge such as H^+, Li^+, and Na^+. However, the following possibility can be considered for case (d): a vacancy of the first-neighbour oxygen OT(1), denoted as $V_{OT(1)}$, plays the role of a divalent positive charge compensator for two Fe^{3+} ions located simultaneously at both Ti(1) and Ti(2). This vacancy model has the advantage that the oxygen vacancy locally compensates the electric charges of the Fe^{3+} substitution. EPR data for the centres C1 and C3 are more similar than those for C2 and C4. This reflects the fact that the shorter Ti(2)–OT(1) bond will be more distorted than the longer Ti(1)–OT(1) bond due to the presence of the oxygen vacancy $V_{OT(1)}$ as a charge compensator.

Acknowledgments

This work was partially supported by the Korea Science and Engineering Foundations through the Research Centre for Dielectric and Advanced Matter Physics at Pusan National University (1997–200). One of the authors (SWA) is grateful to the Korea Research Foundation for a Postdoctoral Fellowship.

References

[1] Tordjman I, Masse R and Guitel J C 1974 *Z. Kristallogr.* **139** 103
[2] Thomas P A, Glazer A M and Watts B E 1990 *Acta Crystallogr.* B **46** 333
[3] Nizamutdinova N M, Khasanova N M, Bulka G R, Vinokurov V M, Rez I S, Garmash V M and Pavlova N I 1987 *Sov. Phys.–Crystallogr.* **32** 408
[4] Stenger J F, Dusausoy Y, Marnier G, Rager H and Gaite J M 1989 *J. Phys.: Condens. Matter* **1** 4643
[5] Gaite J M, Stenger J F, Dusausoy Y, Marnier G and Rager H 1991 *J. Phys.: Condens. Matter* **3** 7877
[6] Ahn S W, Choh S H and Kim J N 1995 *J. Phys.: Condens. Matter* **7** 667
[7] Ahn S W, Choh S H and Choi B C 1995 *J. Phys.: Condens. Matter* **7** 9615
[8] Ahn S W, Choh S H and Rudowicz C 1997 *Appl. Magn. Reson.* **12** 351
[9] Choi B C, Kim J B, Yun S I and Kim J N 1993 *Korean Appl. Phys.* **6** 27
[10] Bolt R J, De Hass H, Sebastian M T and Klapper H 1991 *J. Cryst. Growth* **110** 587
[11] Mombourquette M J, Weil J A and McGavin D G 1994 *Operating Instructions for Computer Program EPR-NMR (Version 6.0)* Department of Chemistry, University of Saskatchewan, Canada
[12] Weil J A, Bolton J R and Wertz J E 1994 *Electron Paramagnetic Resonance* (New York: Wiley) ch 4
[13] Rudowicz C and Bramley R 1985 *J. Chem. Phys.* **83** 5192
[14] Rudowicz C 1986 *J. Chem. Phys.* **84** 5054
[15] Rudowicz C 1987 *Magn. Reson. Rev.* **13** 1
[16] Michoulier J and Gaite J M 1972 *J. Chem. Phys.* **56** 5205
[17] Gaite J M and Michoulier J 1973 *J. Chem. Phys.* **59** 488